Chin. Ann. Math.
36B(5), 2015, 871–882
DOI: 10.1007/s11401-015-0981-x

Chinese Annals of Mathematics, Series B

Transversal Instability for the Thermodiffusive Reaction-Diffusion System*

Michal KOWALCZYK[1] Benoît PERTHAME[2] Nicolas VAUCHELET[2]

(*In Honor of the Scientific Contributions of Professor Luc Tartar*)

Abstract The propagation of unstable interfaces is at the origin of remarkable patterns that are observed in various areas of science as chemical reactions, phase transitions, and growth of bacterial colonies. Since a scalar equation generates usually stable waves, the simplest mathematical description relies on two-by-two reaction-diffusion systems. The authors' interest is the extension of the Fisher/KPP equation to a two-species reaction which represents reactant concentration and temperature when used for flame propagation, and bacterial population and nutrient concentration when used in biology.

The authors study circumstances in which instabilities can occur and in particular the effect of dimension. It is observed numerically that spherical waves can be unstable depending on the coefficients. A simpler mathematical framework is to study transversal instability, which means a one-dimensional wave propagating in two space dimensions. Then, explicit analytical formulas give explicitely the range of paramaters for instability.

Keywords Traveling waves, Stability analysis, Reaction-diffusion equation, Thermodiffusive system
2000 MR Subject Classification 35C07, 70K50, 76E17, 80A25, 92C17

1 Introduction

The propagation of unstable interfaces is at the origin of remarkable patterns that can be observed in nature and in experiments, and the name "cellular instability" is typically used when flame propagation is concerned. The phenomena has attracted the attention of physicists, geophysicists, chemists and biologists and the basic mathematical models can account for this type of unstable dynamical patterns. These models are reaction-diffusion systems and the simplest model is an extension of the Fisher/KPP equation to a two-species reaction. It models reactant concentration and temperature when used for flame propagation (see [2, 4]), bacterial population and nutrient concentration when used in biology (see [8, 13]), cancer cells and available oxygen/glucosis when used for tumor growth (see [1, 14, 16]).

Manuscript received February 12, 2014.
[1]Departamento de Ingenieria Matemática and Centro de Modelamiento Matemático (UMI CNRS 2807), Universidad de Chile, Santiago, Chile. E-mail: kowalczy@dim.uchile.cl
[2]Sorbonne Universités, UPMC Univ Paris 06, UMR 7598, Laboratoire Jacques-Louis Lions, F-75005, Paris, France; CNRS, UMR 7598, Laboratoire Jacques-Louis Lions, F-75005, Paris, France; INRIA-Paris-Rocquencourt, EPC MAMBA, Domaine de Voluceau, BP105, 78153 Le Chesnay Cedex, France. E-mail: benoit.perthame@upmc.fr nicolas.vauchelet@upmc.fr
*This work was supported by the FONDECYT Grant (No. 1130126), the ECOS Project (No. C11E07), the Fondo Basal CMM and the French "ANR Blanche" Project Kibord (No. ANR-13-BS01-0004)

Numerical simulations show that spherical waves can be unstable or stable depending on the model coefficients. But among the many scenarios of instability, the so-called "transversal instabilities" are the simplest to analyze and explain this surprising effect of dimension which is to de-stabilize a stable one-dimensional traveling wave. The phenomena was observed and related to diffusion limited aggregation, with a first analysis in [11, 18].

Our goal here is to study such a case of transversal instability and more precisely, to understand the modalities of appearance of transversal instabilities for a very simple example given by a system. For this, we consider the following two-component reaction-diffusion system:

$$\begin{cases} \partial_t u - \alpha \Delta u = \dfrac{1}{\alpha} h(u) v, \\ \partial_t v - \Delta v = -\dfrac{1}{\alpha} h(u) v. \end{cases} \tag{1.1}$$

The parameter $\alpha > 0$ is called the Lewis number for flame propagation theory, $\alpha > 1$ is relevant for combustion, and $\alpha < 1$ is more relevant for applications to bacterial movement.

Two different cases are proposed for both combustion and biology litteratures depending on the properties of the function $h(\cdot)$

$$h \in C^1(0,1), \quad h(0) = 0, \quad h(1) = 1, \quad h'(u) > 0 \quad \text{for } 0 < u \le 1 \quad \text{(KPP Type)},$$
$$\begin{cases} h(u) = 0 \quad \text{for } 0 \le u \le \theta < 1, \quad h(\theta+) = h^+ \ge 0, \\ h(1) = 1, \quad h'(u) \ge 0 \quad \text{for } \theta < u \le 1 \end{cases} \quad \text{(Ignition Temperature Type)}.$$

Our interest lies in the two-dimensional stability of one dimensional traveling waves for this system. A proof of existence for one-dimensional traveling wave solutions can be found in [12] when $h(\cdot)$ is of KPP type and when $\alpha \ge 1$ for the ignition temperature type. Also, in [2], the authors proved existence of traveling waves when $h(\cdot)$ is of the ignition temperature type with no restriction on α. More recent results for the KPP type, in a cylinder and covering all Lewis numbers, can be found in [9]. An instability result, for an asymptotic regime different from ours, can be found in [7], where the high activation energy limit is considered.

In this paper, we consider a simple example for which we can handle analytical computation. It corresponds to the ignition temperature type and the function h is given by

$$h(u) = \begin{cases} 0 & \text{for } u \le \theta, \\ 1 & \text{for } u > \theta. \end{cases} \tag{1.2}$$

We first report in Section 2, based on numerical simulations, two-dimensional spherical waves which can be unstable for certain coefficients. Then, we build analytically the one-dimensional traveling waves in Section 3. The analytical formulas are fundamental to handling the spectral problem arising in the study of linearized stability of the transversal waves in Section 4.

2 Numerical Observations

In two dimensions, numerical simulations of (1.1)–(1.2) exhibit various behaviours depending on the values of α and θ in $(0,1)$. We present them here as a motivation for our theoretical study.

These simulations are obtained using the finite element method implemented within the software FreeFem++ (see [10]). The computational domain is a disc with radius 4 and we denote by Γ its boundary. At the boundary, Neumann boundary conditions are implemented for both u and v as follows:

$$\partial_\nu u|_\Gamma = 0, \quad \partial_\nu v|_\Gamma = 0,$$

where ν is the outward unit normal. We use a semi-implicit time discretization. Then the resulting system is discretized thanks to P1 finite element method.

The initial given data is

$$u^0 = \mathbf{1}_{\{\sqrt{x^2+y^2} \le 0.4\}}, \quad v^0 = 1 - u^0.$$

The time step is $\mathrm{d}t = 0.0025$ and the number of nodes is 21879. The numerical results are depicted in Figures 1–2 where the computed approximation of u is plotted after several times iterations for different values of the parameters α and θ. Depending on the values of α and θ,

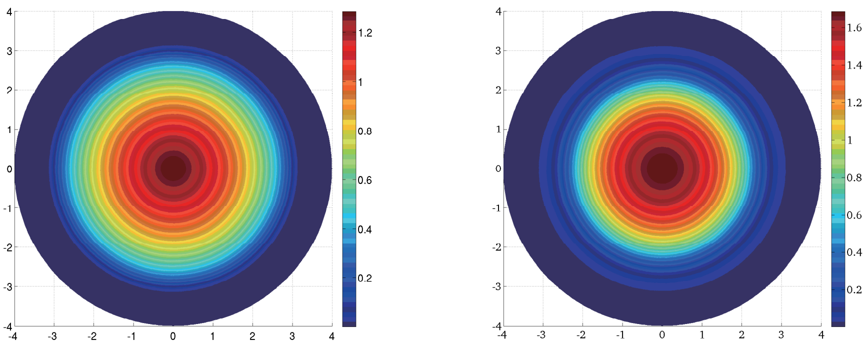

(1) (2)

Figure 1 Numerical simulations for component u in (1.1). (1) Plot of the computed u at time $T = 1$ for $\alpha = 0.25$ and $\theta = 0.1$. (2) Plot of the computed u at time $T = 3$ for $\alpha = 0.25$ and $\theta = 0.5$. In both cases, we observe the propagation of a stable spherical wave which invades the computational domain.

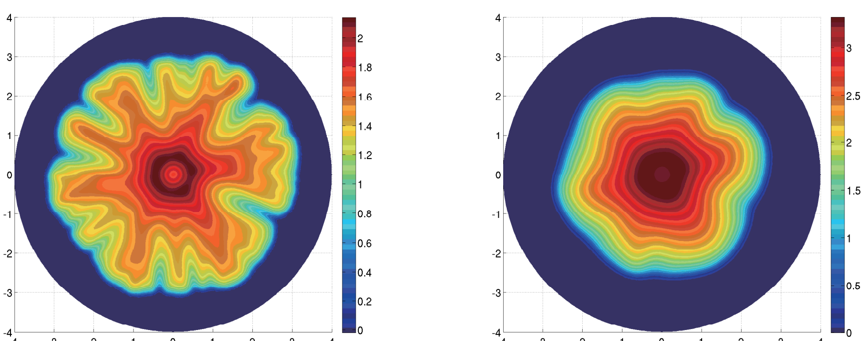

(1) (2)

Figure 2 Numerical simulations for species u in (1.1). (1) Plot of the computed u at time $T = 2$ for $\alpha = 0.01$ and $\theta = 0.1$. (2) Plot of the computed u at time $T = 6$ for $\alpha = 0.25$ and $\theta = 0.5$. When α is small, numerical instabilities appear which create a complex fingered pattern.

we observe different patterns in the numerical simulations. Figure 1 displays the numerical simulations for $\alpha = 0.25$ and for $\theta = 0.1$ (see Figure 1(1)) and $\theta = 0.5$ (see Figure 1(2)). In both cases, we observe a wave that invades the computational domain and the numerical result does not show instabilities. Comparing these two results, we deduce that the invasion process depends on θ. Figure 2 displays the numerical results obtained for small α: We choose $\alpha = 0.01$. In this case, we observe numerical instabilities that create a complex pattern. Instabilities are much more visible when $\theta = 0.1$ (see Figure 2(1)) than when $\theta = 0.5$ (see Figure 2(2)).

3 One-Dimensional Traveling Waves

One-dimensional traveling waves are solutions of the form

$$u(t,x) = u_0(x - \sigma t), \quad v(t,x) = v_0(x - \sigma t),$$

where $\sigma > 0$ is a constant representing the traveling wave velocity. They are a convenient way to understand the propagation phenomena presented in Section 2.

For (1.1) traveling waves are determined from the system

$$\begin{cases} -\sigma u_{0x} - \alpha u_{0xx} = \dfrac{1}{\alpha} h(u_0) v_0, \\ -\sigma v_{0x} - v_{0xx} = -\dfrac{1}{\alpha} h(u_0) v_0, \\ (u_0, v_0)(-\infty) = (1,0), \quad (u_0, v_0)(+\infty) = (0,1). \end{cases} \tag{3.1}$$

To avoid ambiguity due to the translation invariance of the problem, we set

$$0 < u_0(0) = \theta < 1. \tag{3.2}$$

We say that a traveling wave solution to (3.1) is monotonic, if each component is monotonic, and then we can normalize the signs with $u_0' < 0$ and $v_0' > 0$.

Proposition 3.1 *There exists a unique monotonic traveling wave for* (1.1)–(1.2)*, i.e., a unique* $\sigma > 0$ *and a pair* $(u_0, v_0) \in \mathcal{C}^{1,\nu}(\mathbb{R})$*,* $\nu \in (0,1)$*, solving* (3.1)–(3.2) *with* u_0 *nonincreasing, and* v_0 *nondecreasing.*

More precisely, this traveling wave solution moves with the speed

$$\sigma = (1-\theta)\sqrt{\frac{\alpha}{\theta^2 + \alpha\theta(1-\theta)}} \tag{3.3}$$

and is given explicitly by

$$u_0(x) = \begin{cases} 1 - (1-\theta)\mathrm{e}^{\frac{\theta x}{\beta}} & \text{for } x < 0, \\ \theta \mathrm{e}^{-\frac{(1-\theta)x}{\beta}} & \text{for } x > 0, \end{cases} \tag{3.4}$$

$$v_0(x) = \begin{cases} \dfrac{\alpha(1-\theta)}{\theta + \alpha(1-\theta)} \mathrm{e}^{\frac{\theta x}{\beta}} & \text{for } x < 0, \\ 1 - \dfrac{\theta}{\theta + \alpha(1-\theta)} \mathrm{e}^{-\frac{\alpha(1-\theta)x}{\beta}} & \text{for } x > 0, \end{cases} \tag{3.5}$$

where

$$\beta = \sqrt{\alpha\theta}\,\sqrt{\theta + \alpha(1-\theta)}. \tag{3.6}$$

This solution is depicted in Figure 3.

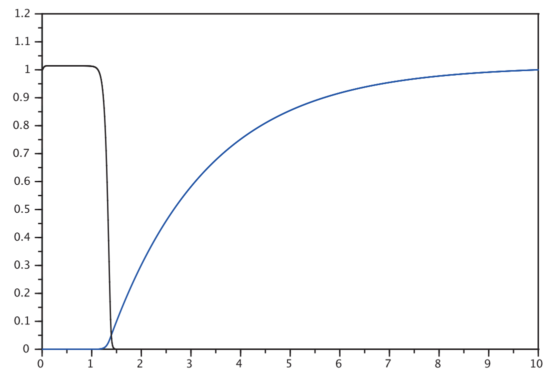

Figure 3 The traveling wave solution with u decreasing and v increasing for $\alpha = 0.005$ and $\theta = 0.1$.

Remark 3.1 We notice that when θ goes to 0, we have $\sigma \sim \frac{\sqrt{\alpha}}{\theta}$. Then the wave goes faster when θ is smaller. This remark confirms our observation in Figure 1, where we can notice that the inversion process of species u is faster when θ is smaller.

Proof of Proposition 3.1 We recall that we look for a nonincreasing function u and we have denoted $u_0(0) = \theta$. Therefore, from the definition of the nonlinearity $h(\cdot)$ in (1.2), we have $h(u_0(x)) = 0$ for $x > 0$. Then, (3.1) is reduced to

$$-\sigma u_{0x} - \alpha u_{0xx} = 0, \quad -\sigma v_{0x} - v_{0xx} = 0, \quad x > 0.$$

With the boundary condition at $+\infty$ in (3.1): $(u_0, v_0)(+\infty) = (0, 1)$, we deduce

$$u_0(x) = \theta \mathrm{e}^{-\frac{\sigma x}{\alpha}}, \quad v_0(x) = 1 - b\mathrm{e}^{-\sigma x} \quad \text{for } x > 0, \tag{3.7}$$

where b is a constant to be fixed later.

For $x < 0$, we have $h(u_0(x)) = 1$, and therefore (3.1) is reduced to

$$-\sigma u_{0x} - \alpha u_{0xx} = \frac{v_0}{\alpha}, \quad \sigma v_{0x} + v_{0xx} - \frac{v_0}{\alpha} = 0.$$

Solving the second equation, because the solution is continuous at $x = 0$ by elliptic regularity, leads to

$$v_0(x) = (1 - b)\mathrm{e}^{\lambda x} \quad \text{with } \lambda = \frac{1}{2}\Big(- \sigma + \sqrt{\frac{\sigma^2 + 4}{\alpha}}\Big) \quad \text{for } x < 0, \tag{3.8}$$

where we have used the boundary conditions $(u_0, v_0)(-\infty) = (1, 0)$. Then, we obtain

$$u_0(x) = 1 - (1 - \theta)\mathrm{e}^{\lambda x} \quad \text{for } x < 0, \tag{3.9}$$

which is a solution to the equation for u_0 provided that

$$(\sigma\lambda + \alpha\lambda^2)(1 - \theta) = \frac{1 - b}{\alpha}.$$

This latter equality allows to determine the value of b as follows:

$$b = 1 - \alpha(1 + \sigma\lambda(1 - \alpha))(1 - \theta).$$

Finally, the continuity of the derivative $u_0'(0^+) = u_0'(0^-)$ implies $\frac{\sigma\theta}{\alpha} = \lambda(1-\theta)$. Using this relation and the expression of λ (3.8), we obtain

$$\sigma = (1-\theta)\sqrt{\frac{\alpha}{\theta^2 + \alpha\theta(1-\theta)}}.$$

We deduce

$$\lambda = \frac{\sqrt{\theta}}{\sqrt{\alpha}\sqrt{\theta+\alpha(1-\theta)}}, \quad \sigma\lambda = \frac{1-\theta}{\theta+\alpha(1-\theta)}, \quad b = \frac{\theta}{\theta+\alpha(1-\theta)}. \tag{3.10}$$

The conclusions stated in Proposition 3.1 follow directly from the construction and formulas (3.7)–(3.9).

4 Stability of Planar Traveling Waves

As suggested by the numerical results in Section 2, based on spherical waves, we expect that transversal instability can occur in two dimensions.

We propose here to study the linear transversal stability. To do so, and in the spirit of [6–7, 11] for instance, with $\varepsilon \ll 1$, we set

$$\begin{cases} u(t,x,y) = u_0(x-\sigma t) + \varepsilon \mathrm{e}^{\lambda t}\cos(\omega y) u_1(x-\sigma t), \\ v(t,x,y) = v_0(x-\sigma t) + \varepsilon \mathrm{e}^{\lambda t}\cos(\omega y) v_1(x-\sigma t). \end{cases}$$

Substituting this expansion into (1.1) and keeping only the term of order 1 in ε, we get the linearized system (in the traveling wave frame)

$$\begin{cases} \lambda u_1 - \sigma u_1' - \alpha u_1'' + \alpha\omega^2 u_1 = \dfrac{1}{\alpha}(h'(u_0)v_0u_1 + h(u_0)v_1), \\ \lambda v_1 - \sigma v_1' - v_1'' + \omega^2 v_1 = -\dfrac{1}{\alpha}(h'(u_0)v_0u_1 + h(u_0)v_1). \end{cases} \tag{4.1}$$

We notice that for $\omega = 0$, the system has the solution $\lambda = 0$, $u_1 = u_0'$ and $v_1 = v_0'$. Notice that $\omega = 0$ also represents the case of dimension one (no transversal effects).

Definition 4.1 *In two dimensions, we say that the one-dimensional traveling wave* (u_0, v_0) *for* (1.1) *in Proposition* 3.1 *is transversally linearly unstable if there exists* $\omega > 0$ *and* λ *with* $\operatorname{Re}\lambda > 0$ *such that* (4.1) *admits a non-trivial solution in* $\mathcal{C}^\nu(\mathbb{R}) \cap L^2(\mathbb{R})$.

Proposition 4.1 *Let* $\theta \in (0,1)$. *Let us consider the function* h *given in* (1.2). *Then the following hold:*

(1) *For* α *small enough, the traveling waves in Proposition* 3.1 *are linearly stable in one dimension for all* $\theta \in (0,1)$.

(2) *For each* $\theta \in (0,1)$ *and each small* α, *there exists* $\omega(\alpha,\theta)$ *such that* $\lambda(\omega(\alpha,\theta)) < 0$, *i.e., the traveling wave is transversally linearly unstable for these values of the parameters in two dimensions. Moreover,* $\omega(\alpha,\theta) = \mathcal{O}(\frac{1}{\sqrt{\alpha}})$.

Sattinger [15] suggested that, in appropriate weighted spaces, one-dimensional traveling waves are nonlinearly stable in the range of parameters when they are linearly stable.

Proof of Proposition 4.1 Since linear stability in one dimension reduces to studying (4.1) for $\omega = 0$, from now on we assume more generally that $\omega \geq 0$. We will look for $\lambda \in \mathbb{R}$,

$\lambda = \lambda(\omega) > 0$ such that (4.1) admits a non-trivial solution. Note that λ depends on α and θ as well, but we will not make this dependence explicit unless necessary.

For $x > 0$, (4.1) reduces to

$$\begin{cases} (\alpha\omega^2 + \lambda)u_1 - \dfrac{(1-\theta)\alpha}{\beta}u_1' - \alpha u_1'' = 0, \\ (\lambda + \omega^2)v_1 - \dfrac{(1-\theta)\alpha}{\beta}v_1' - v_1'' = 0. \end{cases}$$

We can solve this linear problem and obtain

$$\begin{cases} u_1(x) = A\mathrm{e}^{r_- x}, \quad r_- = -\dfrac{(1-\theta)}{2\beta} - \dfrac{1}{2\beta}\sqrt{(1-\theta)^2 + 4\beta^2\Big(\omega^2 + \dfrac{\lambda}{\alpha}\Big)}, \\ v_1(x) = B\mathrm{e}^{s_- x}, \quad s_- = -\dfrac{(1-\theta)\alpha}{2\beta} - \dfrac{1}{2\beta}\sqrt{(1-\theta)^2\alpha^2 + 4\beta^2(\omega^2 + \lambda)}. \end{cases} \tag{4.2}$$

Here, A and B are constants to be determined and $r_\pm$ are the roots of the polynomial

$$(\alpha\omega^2 + \lambda) - \frac{(1-\theta)\alpha}{\beta}r - \alpha r^2 = 0. \tag{4.3}$$

For $x < 0$, (4.1) reduces to

$$\begin{cases} (\alpha\omega^2 + \lambda)u_1 - \dfrac{(1-\theta)\alpha}{\beta}u_1' - \alpha u_1'' = \dfrac{1}{\alpha}v_1, \\ \Big(\lambda + \omega^2 + \dfrac{1}{\alpha}\Big)v_1 - \dfrac{(1-\theta)\alpha}{\beta}v_1' - v_1'' = 0, \end{cases}$$

where we have used the expression of σ in (3.3) recalling that β is given in (3.6). Then we get

$$v_1(x) = B\mathrm{e}^{\mu_+ x}, \quad \mu_+ = -\frac{(1-\theta)\alpha}{2\beta} + \frac{1}{2\beta}\sqrt{(2\theta + \alpha(1-\theta))^2 + 4\beta^2(\omega^2 + \lambda)}. \tag{4.4}$$

Substituting this expression in the equation for u_1, we get

$$u_1(x) = C\mathrm{e}^{r_+ x} + \gamma B\mathrm{e}^{\mu_+ x}, \quad r_+ = -\frac{(1-\theta)}{2\beta} + \frac{1}{2\beta}\sqrt{(1-\theta)^2 + 4\beta^2\Big(\omega^2 + \frac{\lambda}{\alpha}\Big)}, \tag{4.5}$$

where C is a constant and we have set

$$\Big(\alpha\omega^2 + \lambda - \frac{(1-\theta)\alpha}{\beta}\mu_+ - \alpha\mu_+^2\Big)\gamma = \frac{1}{\alpha}.$$

The value of the parameter γ follows from the definition of $r_\pm$ as the roots of (4.3)

$$\gamma = -\frac{1}{\alpha^2(\mu_+ - r_+)(\mu_+ - r_-)}. \tag{4.6}$$

Moreover, by continuity at $x = 0$, we need $C + B\gamma = A$. By definition of the function h and with (3.4)–(3.5), we obtain

$$h'(u_0)v_0 = \frac{\beta\alpha}{\theta(\theta + \alpha(1-\theta))}\delta_{x=0} = \frac{\alpha^2}{\beta}\delta_{x=0}. \tag{4.7}$$

As a consequence, the jump relation for (u_1', v_1') at $x = 0$, which can be deduced from (4.1), leads to

$$\begin{cases} -\alpha(u_1'(0^+) - u_1'(0^-)) = \dfrac{\alpha}{\beta} u_1(0), \\ -v_1'(0^+) + v_1'(0^-) = -\dfrac{\alpha}{\beta} u_1(0). \end{cases}$$

Writing these equalities in terms of the free parameters, we arrive at the following set of relations:

$$\begin{cases} A = C + \gamma B, \\ A\Big(r_- + \dfrac{1}{\beta}\Big) = C r_+ + \gamma \mu_+ B, \\ \dfrac{\alpha}{\beta} A = B s_- - B\mu_+. \end{cases}$$

Replacing B and C in the second equation, we get

$$A\Big(r_- + \frac{1}{\beta}\Big) = A r_+ + A\gamma(\mu_+ - r_+)\frac{\alpha}{\beta(s_- - \mu_+)}.$$

We conclude that there exists a non trivial solution to (4.1) provided that the following identity holds:

$$1 = \beta(r_+ - r_-) + \frac{1}{\alpha(\mu_+ - r_-)(\mu_+ - s_-)}, \tag{4.8}$$

where we used the expression (4.6). We verify straightforwardly that for $\omega = 0$ and $\lambda = 0$, (4.8) is always satisfied.

It remains to compute the value of λ using (4.8). In this algebraic equation, λ is given implicitly as a function of the parameters α, θ and ω, and in the analysis of this expression, we rely on taking the limit $\alpha \to 0$ and also on Maple-based simulations (in this sense our proof is to some small extent computer-assisted).

First, we consider the case $\omega = 0$ which provides the stability in one dimension. Then we consider the limit $\alpha \to 0$ choosing the scale $\omega = \frac{\omega_0}{\sqrt{\alpha}}$, with $\omega_0 > 0$ fixed.

Case 1 $\alpha \to 0$, $\omega = 0$. This case covers the assertion (1) of the proposition. We set

$$\zeta = \sqrt{(1-\theta)^2 + \frac{4\beta^2\lambda}{\alpha}}, \quad \eta = \sqrt{(2\theta + \alpha(1-\theta))^2 + 4\beta^2\lambda}.$$

Using (4.2) and (4.4)–(4.5), the identity (4.8) in the case $\omega = 0$ reduces to

$$1 = \zeta + \frac{4\beta^2}{\alpha((1-\theta)(1-\alpha) + \zeta + \eta)(\eta + \alpha\zeta)}. \tag{4.9}$$

Taking $\alpha = 0$ above, we find

$$\lambda = -\frac{1}{2}\frac{1-\theta}{\theta}.$$

By continuity, this means in particular that for all sufficiently small α, the traveling wave solution is linearly stable. Hence, it is tempting to speculate that in fact linear stability is true for any $\alpha > 0$, see however Remark 5.2.

Case 2 $\alpha \to 0$ and $\omega = \frac{\omega_0}{\sqrt{\alpha}}$. Calculations are quite similar in this case. Denoting now

$$\zeta = \sqrt{(1-\theta)^2 + 4\theta^2(\lambda + \omega_0^2)},$$

we need to solve

$$1-\zeta = \frac{2\theta}{(\sqrt{\omega_0^2+1}+\omega_0)(1-\theta+2\theta\sqrt{\omega_0^2+\zeta})}.$$

Therefore,

$$\zeta = \frac{1}{2}\Big(\theta - 2\theta\sqrt{\omega_0^2+1} + \sqrt{\Big(\theta-2\theta\sqrt{\omega_0^2+1}\Big)^2 + 4 - 4\theta + 8\theta\omega_0}\Big)$$

and then

$$\lambda = -\omega_0^2 + \frac{1}{16\theta^2}\Big(\theta - 2\theta\sqrt{\omega_0^2+1} + \sqrt{\Big(\theta-2\theta\sqrt{\omega_0^2+1}\Big)^2 + 4 - 4\theta + 8\theta\omega_0}\Big)^2 - \Big(\frac{1-\theta}{2\theta}\Big)^2.$$

In this case, depending on the value of ω_0, we may have $\lambda > 0$ or $\lambda < 0$. Figure 4 illustrates the situation.

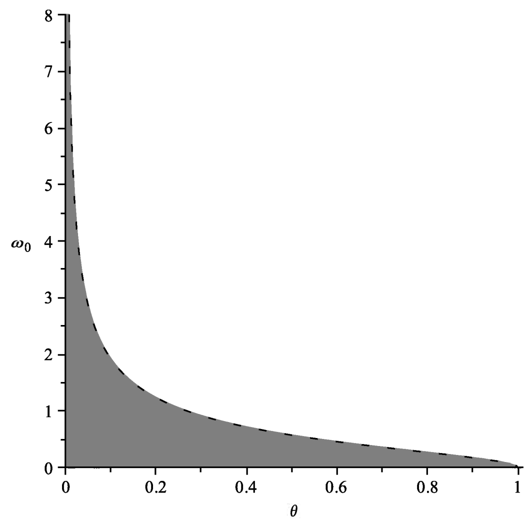

Figure 4 Plot of the region of instability $\lambda = \lambda(\theta, \omega_0) > 0$, shaded.

5 Concluding Remarks

Remark 5.1 It has been noted with the numerical simulations of Section 2, that for small values of α, instabilities are more visible when θ is small (see Figure 2). The plot of the region of instability in Figure 4 confirms this observation. In fact, we notice on this latter figure that small values of θ allows large values of ω_0 which can be seen as a frequency of oscillations in the transversal direction.

Remark 5.2 We use (4.9) and denote

$$F(\alpha,\theta,\lambda) = \zeta + \frac{4\beta^2}{\alpha((1-\theta)(1-\alpha)+\zeta+\eta)(\eta+\alpha\zeta)} - 1.$$

Solutions to $F(\alpha,\theta,\lambda) = 0$ determine the eigenvalues $\lambda = \lambda(\alpha,\theta)$. It is easy to check that

$$\lim_{\alpha\to\infty} F(\alpha,\theta,\lambda) = \infty, \quad \forall\lambda > 0,\ \theta \in (0,1),$$

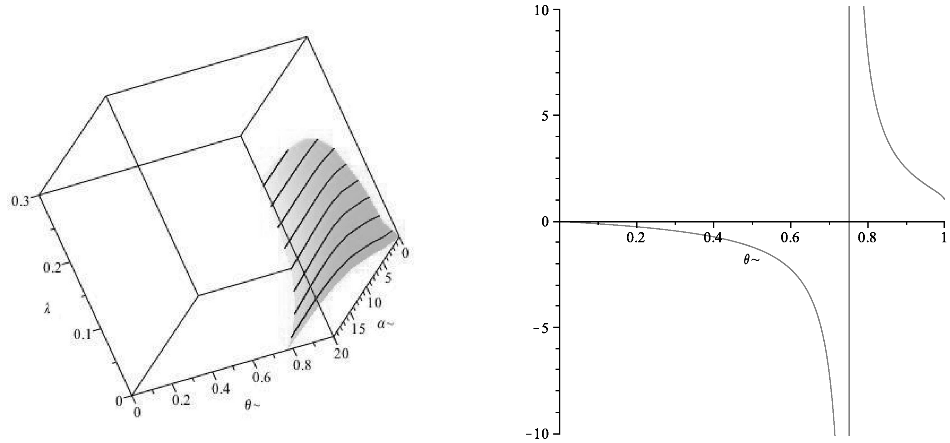

(1) (2)

Figure 5 (1) Plot of the level set $F(\alpha, \theta, \lambda) = 0$. (2) Plot of the implicitly defined curve $\theta \mapsto \alpha(\theta)$ where $F(\alpha(\theta), \theta, 0) = 0$. It suggests that the instability appears for some $\theta^* \in (0.7, 0.8)$ and the corresponding values of α are larger than 1. This is confirmed by a more refined analysis of the picture on the right.

however, this limit is not uniform. Indeed there exists a θ^* such that for any $\theta \in (\theta^*, 1)$ we can find a value $\alpha(\theta) > 0$ such that $F(\alpha, \theta, \lambda) = 0$ for some $\lambda > 0$. We illustrate this in Figure 5.

The fact that the traveling wave in one dimension is unstable for large values of the Lewis number is somewhat a surprise and raises a more general question of stability or instability for the problems with KPP-type or ignition-type nonlinearities. Note that, in both cases, we are dealing with a prey-predator system and in particular, the linear problem is non-cooperative. This means that methods based on the maximum principle do not work and the known results (see for instance [19]) do not apply. The special feature of our problem is the monotonicity of the traveling fronts. With this property, one may expect that they should be stable, as it happens for scalar problems and is seen easily there from the Krein-Rutman theorem. For systems of equations, there is no general theory that one could apply but monotone waves are stable in some cases (see for instance [3]). Our example shows that the question is in fact more subtle.

Remark 5.3 Writing (4.8) in the form

$$0 = -1 + \beta(r_+ - r_-) + \frac{1}{\alpha(\mu_+ - r_-)(\mu_+ - s_-)},$$

we obtain a dispersion relation $\lambda = \lambda(\omega)$ for any fixed α and θ. Pictures in Figure 6 confirm the intuitively obvious fact that there should always be the most unstable frequency ω^*, that is, a maximum value of λ relevant to Turing instability.

The intention of this note is to shed some light on the mechanism of the onset of instability of traveling waves in higher dimension, and in particular to get some ideas about the shape of the dispersion curves for more general problems of the KPP and the ignition type. We chose to study the planar waves for a simple problem where explicit solutions are available since, unlike

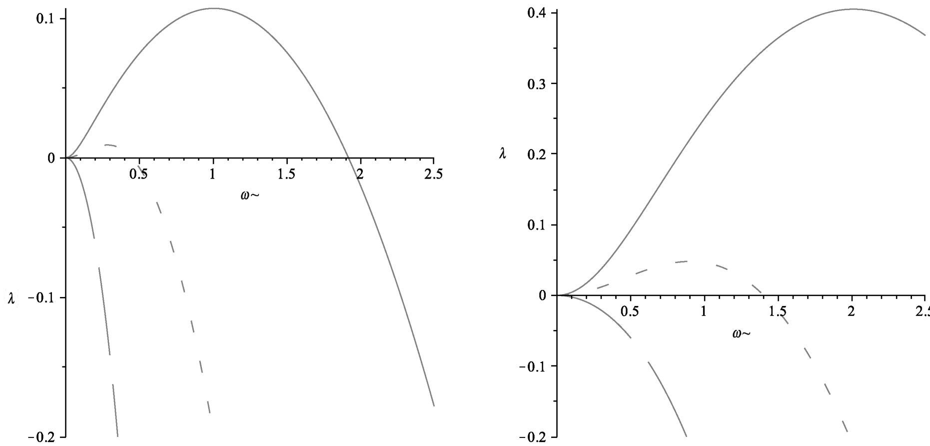

(1) (2)

Figure 6 (Left) Plot of the dispersion curve $\lambda(\omega)$ for $\theta = 0.4$ and $\alpha = 0.1$ (continuous line), $\alpha = 0.4$ (dotted line) and $\alpha = 1.3$ (dashed line). (Right) Plot of the dispersion curve for $\theta = 0.1$ and $\alpha = 0.1$ (continuous line) $\alpha = 0.2$ (dotted line) $\alpha = 0.4$ (dashed line).

for example in the case of some activator-inhibitor systems (see [5, 17–18]), there does not seem to exist a well-established methodology to deal with this issue. Indeed, the usual approach, involving some limit procedure, is based on the fact that of one of the components of the system becomes more concentrated in space, for example, it has a form of a spike or undergoes a sharp transition, as the small parameter tends to 0. This leads in many cases to a limiting problem for which the spectrum can be completely understood. However, for the KPP or ignition type nonlinearities it is not immediately clear what the limiting problem should be. We believe that the instability of the planar fronts described here is a robust phenomenon with respect to the change of the nonlinearities.

References

[1] Ben Amar, M. and Goriely, A., Growth and instability in elastic tissues, *J. Mech. Phys. Solids*, **53**(10), 2005, 2284–2319.

[2] Berestycki, H., Nicolaenko, B. and Scheurer, B., Traveling wave solutions to combustion models and their singular limits, *SIAM J. Math. Anal.*, **16**(6), 1985, 1207–1242.

[3] Berestycki, H., Terracini, S., Wang, K. L. and Wei, J. C., On entire solutions of an elliptic system modeling phase separations, *Adv. Math.*, **243**, 2013, 102–126.

[4] Billingham, J. and Needham, D. J., The development of travelling waves in quadratic and cubic autocatalysis with unequal diffusion rates I, Permanent form travelling waves, *Philos. Trans. Roy. Soc. London Ser. A*, **334**(1633), 1991, 1–24.

[5] Chen, X. and Taniguchi, M., Instability of spherical interfaces in a nonlinear free boundary problem, *Adv. Differential Equations*, **5**(4–6), 2000, 747–772.

[6] Ciarletta, P., Foret, L. and Ben Amar, M., The radial growth phase of malignant melanoma: Multi-phase modelling, numerical simulation and linear stability, *J. R. Soc. Interface*, **8**(56), 2011, 345–368.

[7] Glangetas, L. and Roquejoffre, J.-M., Bifurcations of travelling waves in the thermo-diffusive model for flame propagation, *Arch. Rational Mech. Anal.*, **134**, 1996, 341–402.

[8] Golding, I., Kozlovsky, Y., Cohen, I. and Ben Jacob, E., Studies of bacterial branching growth using reaction-diffusion models for colonial development, *Physica A*, **260**, 1998, 510–554.

[9] Hamel, F. and Ryzhik, L., Traveling fronts for the thermo-diffusive system with arbitrary Lewis numbers, *Arch. Ration. Mech. Anal.*, **195**(3), 2010, 923–952.

[10] Hecht, F., New development in freefem++, *J. Numer. Math.,* **20**(3–4), 2012, 251–265.

[11] Kessler, D. A. and Levine, H., Fluctuation-induced diffusive instabilities, *Letters to Nature,* **394**, 1998, 556–558.

[12] Marion, M., Qualitative properties of a nonlinear system for laminar flames without ignition temperature, *Nonlinear Anal.,* **9**(11), 1985, 1269–1292.

[13] Mimura, M., Sakaguchi, H. and Matsushita, M., Reaction diffusion modelling of bacterial colony patterns, *Physica A,* **282**, 2000, 283–303.

[14] Perthame, B., Quirós, F. and Vázquez, J. L., The Hele-Shaw asymptotics for mechanical models of tumor growth, *ARMA,* **212**, 2014, 93–127.

[15] Sattinger, D. H., On the stability of waves of nonlinear parabolic systems, *Advances in Math.,* **22**(3), 1976, 312–355.

[16] Sherratt, J. A. and Chaplain, M. A. J., A new mathematical model for avascular tumour growth, *J. Math. Biol.,* **43**(4), 2001, 291–312.

[17] Taniguchi, M., Instability of planar traveling waves in bistable reaction-diffusion systems, *Discrete Contin. Dyn. Syst. Ser. B,* **3**(1), 2003, 21–44.

[18] Taniguchi, M. and Nishiura, Y., Instability of planar interfaces in reaction-diffusion systems, *J. Numer. Math.,* **25**(1), 1994, 99–134.

[19] Volpert, A. I., Volpert, V. A. and Volpert, V. A., Traveling wave solutions of parabolic systems, Translations of Mathematical Monographs (translated from the Russian manuscript by James F. Heyda), Vol. 140, A. M. S., Providence, RI, 1994.